BIOCHEMISTRY
including biophysical chemistry & molecular biology
Article

Biochemistry **2009,** *48,* 6551–6558 6551
DOI: 10.1021/bi9006644

Characterization of an Aldolase−Dehydrogenase Complex That Exhibits Substrate Channeling in the Polychlorinated Biphenyls Degradation Pathway†

Perrin Baker,‡ Dan Pan,‡ Jason Carere, Adam Rossi, Weijun Wang, and Stephen Y. K. Seah*

Department of Molecular and Cellular Biology, University of Guelph, Guelph, Ontario, Canada ‡*These authors contributed equally to this work*

Received April 17, 2009; Revised Manuscript Received May 27, 2009

ABSTRACT: An aldolase and dehydrogenase complex from the polychlorinated biphenyl degradation pathway of the bacterium *Burkholderia xenovorans* LB400 was purified. The aldolase, BphI, had the highest activity with Mn^{2+} as the cofactor and was able to transform 4-hydroxy-2-oxopentanoate and 4-hydroxy-2-oxohexanoate to pyruvate and acetaldehyde or propionaldehyde with similar specificity constants. Aldolase activity was competitively inhibited by the pyruvate enolate analogue, oxalate, with a K_{ic} of 0.93 μM. The pH−rate profiles suggested the involvement of a pK_a 7.7 catalytic base in the reaction mechanism. BphI activity was activated 15-fold when substrate turnover was occurring in the dehydrogenase, BphJ, which can be attributed partially to nicotinamide coenzyme binding to BphJ. BphJ had similar specificity constants for acetaldehyde or propionaldehyde and was able to utilize aliphatic aldehydes from two to five carbons in length as substrates, although K_m values for these aldehyes were >20 mM. When 4-hydroxy-2-oxopentanoate was provided as a substrate to the BphI−BphJ complex in a coupled enzyme assay, no lag in the progress curve of BphJ was observed. When 1 mM propionaldehyde was added exogenously to a reaction mixture containing 0.1 mM 4-hydroxy-2-oxopentanoate, 95% of the CoA esters produced was acetyl CoA. Conversely, 99% of the CoA esters produced was propionyl CoA when a 10-fold molar excess of exogenous acetaldehyde was added in a reaction mixture containing 4-hydroxy-2-oxohexanoate. These results demonstrate that acetaldehyde and propionaldehyde, products of the BphI reaction, are not released in the bulk solvent but are channeled directly to the dehydrogenase.

The *meta* cleavage pathway is an important metabolic route for the aerobic degradation of diverse aromatic compounds by bacteria. In *Mycobacterium tuberculosis*, this pathway is a potential target for development of antituberculosis drugs as it enables the bacteria to catabolize membrane cholesterol, providing carbon and energy sources for their survival in host-activated macrophages (*1*−*3*). In other bacteria, this pathway can be exploited for bioremediation of recalcitrant industrial aromatic pollutants, such as benzene, phenol, and polychlorinated biphenyls (PCBs) (*4*−*7*).

Transformation of aromatic compounds via the *meta* cleavage pathway leads to the formation of the common metabolite, 4-hydroxy-2-ketoacid, which undergoes carbon−carbon bond cleavage, to form pyruvate and an aldehyde (Scheme 1). Interestingly, this reaction is catalyzed by two evolutionarily distinct divalent metal-dependent pyruvate aldolases in the *meta* cleavage pathway. The aldolase, HpaI, from the catabolic pathway for 3- and 4-hydroxyphenylacetate in *Escherichia coli* strain W or C belongs to the pyruvate/phosphoenolpyruvate family of enzymes, whose members also include isocitrate lyase and pyruvate kinase (*8*, *9*). BphI, the pyruvate aldolase from the PCB degradation pathway of *Burkholderia xenovorans* LB400, on the other hand, belongs to the HMGL family of enzymes that includes 3-hydroxy-3-methylglutaryl-CoA lyase, 2-isopropylmalate synthase, and transcarboxylase 5S (*10*). Biochemical characterization of HpaI has yielded important information regarding its structure, substrate specificity, and catalytic mechanism (*11*−*13*). In contrast, little biochemical work has been performed on BphI or its homologues. Thus, kinetic parameters and substrate specificity have never been determined. The crystal structure of the aldolase, DmpG, from the phenol degradation pathway of *Pseudomonas* sp. CF600, which is ~50% identical in sequence to BphI, shows that this TIM barrel enzyme forms a complex with the next enzyme in the pathway, DmpF, an acylating aldehyde dehydrogenase. The aldehyde dehydrogenase catalyzes the conversion of the acetaldehyde product of the aldolase to acetyl CoA, using NAD^+ and coenzyme A as cofactors. The structure of DmpG−DmpF complex also shows a small internal tunnel that can

†This research is supported by National Science and Engineering Research Council of Canada (NSERC) Grant 238284 (to S.Y.K.S.). P. B. and A.R. are recipients of a NSERC PGS-D scholarship and a USRA studentship, respectively.

*To whom correspondence should be addressed: Department of Molecular and Cellular Biology, University of Guelph, Guelph, Ontario, Canada N1G 2W1. E-mail: sseah@uoguelph.ca. Phone: (519) 824-4120, ext. 56750. Fax: (519) 837-1802.

Published on Web 05/28/2009

Scheme 1: Reaction Catalyzed by an Aldolase from the *Meta* Cleavage Pathway

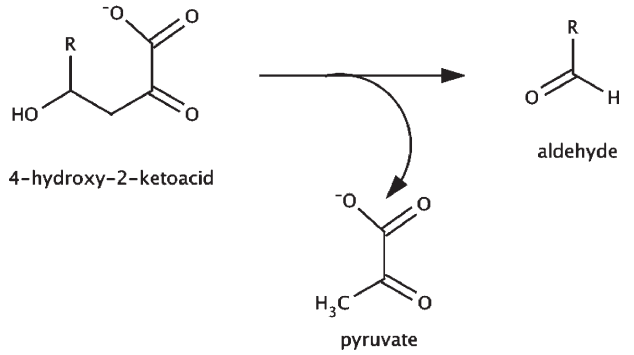

potentially link the active sites of the two enzymes (*14*). This tunnel is bound predominantly by highly conserved, hydrophobic residues, indicating the possibility that the reactive and volatile aldehyde product of the aldolase reaction is not released to the bulk solvent but is directly channeled to the dehydrogenase. In the structure, this tunnel is blocked at the entrance by a tyrosine residue in DmpG (Y291), and although a rotation of the tyrosyl side chain might open the tunnel, it is unclear if substrate channeling actually occurs since it has not been biochemically demonstrated. There is also no reported detailed kinetic characterization of the DmpG−DmpF complex.

Here we describe the expression and purification of the BphI−BphJ complex from the PCB degrader, *B. xenovorans* LB400. Kinetic analyses of the BphI−BphJ complex described here provide the first insights into the substrate specificity, mechanism, allosteric regulation, and substrate channeling in this aldolase and dehydrogenase family of enzymes.

EXPERIMENTAL PROCEDURES

Chemicals. Sodium pyruvate, sodium oxalate, acetaldehyde, propionaldehyde, butyraldehyde, isobutyraldehyde, pentaldehyde coenzyme A, L-lactate dehydrogenase (LDH,[1] rabbit muscle), alcohol dehydrogenase (*Saccharomyces cerevisiae*), and Chelex 100 were from Sigma-Aldrich (Oakville, ON). Restriction enzymes, T4 DNA ligase, and Pfx polymerase were from Invitrogen (Burlington, ON) or New England Biolabs (Pickering, ON). Ni-NTA Superflow resin was obtained from Qiagen (Mississauga, ON). All other chemicals were analytical grade and were obtained from Sigma-Aldrich and Fisher Scientific (Nepean, ON).

DNA Manipulation. DNA was purified, digested, and ligated using standard protocols (*15*). The *bphI* gene was amplified by PCR using the primers GGGGCATATGAAGCTAGAAGGC and GGCCTGCAGTCATGCGGCGGTCAAGG and *bphJ* with the primers CCCCCATATGACGAAAAAAATC and GGGGAAGCTTCAGGCGTGGACGGG. Introduced *Nde*I, *Hin*dIII, and *Pst*I restriction sites are underlined. The PCR mixture contained 10 ng of plasmid template pDD5301 (*16*), 0.8 unit of *Pfx* polymerase (Invitrogen), 20 nM amounts of each dNTP, and 100 pmol of each primer in a total volume of 100 μL. The following amplification profile was followed: 94 °C for 2 min, followed by 30 cycles at 94 °C for 30 s, 50 °C for 30 s, and 68 °C for 1 min, and finally 68 °C for 10 min. The *bphI* fragment was digested with *Nde*I and *Pst*I and ligated into plasmid vector pT7-7 (*17*). The T7 promoter and ribosomal binding site from this vector together with the *bphI* gene were then transferred using restriction sites *Bsr*BI and *Hin*dIII to the broad host range vector, pBTL4 (*18*). *bphJ* on the other hand was inserted into pET28a (EMD, Biosciences Inc., San Diego, CA) using *Nde*I and *Hin*dIII restriction sites. Genes from positive clones were sequenced at the Guelph Molecular Supercenter (University of Guelph). The cloned *bphJ* gene incurred a mutation which was corrected using the Quikchange (Stratagene) site specific mutagenesis method. The *bph*I sequence corresponds to the published sequence from plasmid pDD5301 (*16*), except for a difference in the codon for amino acid 263, which is GCC (Ala) in our sequence and TCC (Ser) in the published sequence. However, the more recently determined *bph*I gene sequence from the *B. xenovorans* LB400 genome sequencing project showed a GCC codon at this position (*19*), consistent with the sequence we obtained.

Preparation of Aldolase Substrates. The aldolase (HpaI) was purified according to the previously reported procedure (*12*). 4-Hydroxy-2-oxopentanoate, 4-hydroxy-2-oxohexanoate, and 4-hydroxy-2-oxoheptanoate were generated enzymatically from pyruvate and acetaldehyde, propionaldehyde, and butyraldehyde, respectively, using purified HpaI. Briefly, 1.107 g of sodium pyruvate and 5 mL of pure aldehyde were mixed with 40 μg of HpaI in a total of 50 mL of 100 mM HEPES buffer (pH 8.0) containing 0.2 mM $CoCl_2$. After 24 h, the cobalt was removed by incubation with 0.5 g of Chelex 100 for 15 min, followed by centrifugation at 12096*g* for 10 min to remove Chelex 100. HpaI was removed by ultrafiltration using an Amicon YM10 filter (Millipore, Nepean, ON), and excess aldehyde was evaporated using a rotovap prior to lyophilization. The concentrations of the respective substrates were determined by coupling their aldol cleavage by excess HpaI with L-lactate dehydrogenase (LDH).

Purification of the BphI−BphJ Complex. Recombinant *E. coli* BL21(λDE3) harboring the *bphI* and *bphJ* genes was propagated in 1 L of Luria-Bertani medium supplemented with 15 μg/mL tetracycline and 34 μg/mL kanamycin at 37 °C. When the optical density reached 0.6−0.8 at a wavelength of 600 nm, 1 mM IPTG was added and the culture was incubated overnight at 15 °C with shaking and then harvested by centrifugation at 12096*g* for 10 min.

The cell pellet was resuspended in 20 mM sodium HEPES (pH 8.5) and disrupted by being passed through a French press three times at an operating pressure of 12000 psi. The cell debris was removed by centrifugation at 39191*g* for 30 min. Phosphate buffer (50 mM) containing 300 mM NaCl (pH 8.0) was used in affinity chromatography unless indicated otherwise. The clear supernatant was filtered through a 0.45 μm filter and incubated for 60 min at 4 °C with the Ni^{2+}-NTA resin in buffer containing 20 mM imidazole. The mixture was poured into a column and washed with 20 mL of buffer containing 20 mM imidazole. The BphI−BphJ complex was eluted with 13 mL of buffer containing 150 mM imidazole. Fractions were pooled, and the buffer was changed to 50 mM sodium phosphate buffer (pH 7.4) by repeated dilution in a stirred cell containing a YM10 filter (Amicon). The histidine tag was removed by cleavage with thrombin. Approximately 2 mg of BphI−BphJ complex in 1 mL aliquots was incubated for 75 min at 25 °C with 11% glycerol and 1 unit of thrombin. Thrombin and uncleaved His-tagged protein were removed using *p*-aminobenzamidine-agarose and Ni^{2+}-NTA

[1]Abbreviations: HEPES, 4-(2-hydroxyethyl)-1-piperazinepropanesulfonic acid; IPTG, isopropyl β-D-thiogalactopyranoside; LDH, L-lactate dehydrogenase; MOPS, 3-(*N*-morpholino)propanesulfonic acid; NMR, nuclear magnetic resonance.

resin, respectively. The enzyme was aliquoted and stored at −80 °C in 20 mM sodium HEPES buffer (pH 8.5) containing 10 mM DTT.

Determination of Protein Concentrations, Purities, and Molecular Masses. Protein concentrations were determined by the Bradford assay (*20*) using bovine serum albumin as the standard. Sodium dodecyl sulfate−polyacrylamide gel electrophoresis (SDS−PAGE) was performed, and the gels were stained with Coomassie Blue according to established procedures (*21*). The BenchMark Protein Ladder (Invitrogen) containing proteins ranging from 10 to 220 kDa was used for molecular mass markers. The native molecular mass of the purified BphI−BphJ complex was estimated using gel filtration on a calibrated HiLoad 26/60 Superdex 200 column (GE Healthcare). The proteins used for calibration were horse heart cytochrome *c* (12.4 kDa), bovine erythrocyte carbonic anhydrase (29 kDa), bovine serum albumin (66 kDa), yeast alcohol dehydrogenase (150 kDa), and sweet potato β-amylase (200 kDa). The void volume was determined using blue dextran (2000 kDa). Chromatography was conducted at 25 °C using 20 mM HEPES buffer (pH 7.5) containing 150 mM NaCl, at a flow rate of 2 mL/min.

Assays for BphI. Aldolase activity was deduced by assessing the production of pyruvate by coupling with NADH oxidation using LDH in a spectrophotometric assay. All assays were performed in at least duplicate in a total volume of 1 mL of 100 mM sodium HEPES buffer (pH 8.0) at 25 °C, using a Varian Cary 3 spectrophotometer equipped with a thermojacketed cuvette holder, and were initiated by adding 2 μg of BphI−BphJ complex, unless otherwise stated. The extinction coefficient of NADH at 340 nm was taken to be 6200 M^{-1} cm^{-1}. A standard aldolase activity assay contained 4 mM substrate, 0.4 mM NADH, 1 mM $MnCl_2$, and 19.2 units of LDH (pH 8.0). The background rate was determined prior to addition of the BphI−BphJ complex and subtracted from the assays containing enzyme. One unit of enzyme represents the amount of protein that produces 1 μmol of pyruvate from substrate in 1 min.

The metal ion specificity of the aldolase was determined by incubating 10 μg of apo-BphI−BphJ complex with 0.1 and 1 mM metal chloride for 5 min followed by activity measurements using the standard continuous assay. The sodium HEPES buffer and the substrate 4-hydroxy-2-oxopentanoate used in the assay were treated with Chelex 100 for 30 min to remove any metal ion contaminants.

Kinetic parameters of the aldolase in the presence of 0.4 mM NADH were determined by the standard continuous assay with the substrate concentration varied from $0.1K_m$ to $10K_m$. Inhibition of the aldolase by oxalate was also assessed using the standard continuous assay with oxalate concentrations varied from $0.2K_i$ to $4K_i$. Kinetic parameters for the aldolase in the absence of BphJ coenzymes or in the presence of NAD^+, $NADP^+$, or CoA were determined using a discontinuous assay which contained 1 mM $MnCl_2$, 80 μg of enzyme, and varying concentrations of 4-hydroxy-2-oxopentanoate in 8 mL of buffer. Coenzymes were added to a final concentration of 0.4 mM with the exception of $NADP^+$ which was added at a final concentration of 2 mM, given the high K_m for this coenzyme. At 2 min intervals, for a duration of 6 min, 918 μL aliquots of the reaction mixture were removed and the reactions quenched with 20 mM EDTA (pH 8.5) and 0.4 mM NADH. The amount of pyruvate produced at each time point was determined by an end point assay by coupling to the stoichiometric oxidation of NADH by LDH. Linear regression was used to determine the reaction velocity for each substrate concentration. Data were fitted by nonlinear regression to the Michaelis−Menten equation using Leonora (*22*).

The activity of BphI, determined when BphJ was undergoing aldehyde turnover, was determined in a discontinuous assay containing 4 mM 4-hydroxy-2-oxopentanoate, 1 mM $MnCl_2$, 0.4 mM NAD^+, and 0.1 mM CoA in a total of 16 mL of 100 mM buffer. Under this condition, BphJ will turn over the acetaldehyde produced from the BphI reaction, and CoA will be the limiting substrate. A solution without enzyme acted as a negative control. At 1 min intervals, the reaction of a 918 μL aliquot of the mixture was quenched by addition of 20 mM EDTA (pH 8.5) and 0.4 mM NADH. The amount of pyruvate produced by BphI was determined by an end point assay by coupling to the stoichiometric oxidation of NADH by LDH.

The effects of pH on the K_m and k_{cat} values of aldolase activity were determined from pH 6.5 to 9.0 in a three-component constant-ionic strength buffer containing 0.1 M Tris, 0.05 M acetic acid, and 0.05 M 2-(*N*-morpholino)ethanesulfonic acid. Data were plotted using eq 1 below by nonlinear regression in Leonora.

$$v = C/(1 + H/K_{a1}) \quad (1)$$

where C is the pH-independent value of k_{cat}/K_m, H is the proton concentration, and K_{a1} is the ionization constant of groups involved in the reaction.

Assays for BphJ. Substrate specificity of the dehydrogenase was determined using 0.4 mM NAD^+, 0.1 mM coenzyme A, and aldehyde concentrations varied from at least $0.1K_m$ to $5K_m$. Concentrations of aldehyde stocks were determined by coupling it to NADH oxidation with alcohol dehydrogenase. Cofactor specificities were determined under similar conditions in which the acetaldehyde concentration was held at 100 mM and the NAD^+ or $NADP^+$ concentration was varied.

Test of Substrate Channeling. The progress curve for BphJ was determined spectrophotometrically at 340 nm, by assessing the reduction of NAD^+ to NADH. The assay contained 0.1 mM 4-hydroxy-2-oxopentanoate, 1 mM $MnCl_2$, 0.4 mM NAD^+, and 0.1 mM CoA in a total of 1 mL of 100 mM sodium HEPES (pH 8.0). In the absence of channeling, the theoretical progress curve for BphJ, assuming there are no limiting substrate concentrations, can be simulated by the following equation (*23*):

$$[NADH] = v_1 t + (v_1/v_2)K_m(e^{-v_2 t/K_m} - 1) \quad (2)$$

where K_m is the Michealis constant for acetaldehyde, v_1 is the rate (micromolar per minute) of the reaction catalyzed by BphI, and v_2 is the rate (micromolar per minute) of the reaction catalyzed by BphJ at near-saturating concentrations of substrates. The K_m/v_2 value indicates the lag time that precedes attainment of the steady-state concentration of aldehyde.

Competition assays contained 0.1 mM 4-hydroxy-2-oxopentanoate or 4-hydroxy-2-oxohexanoate, 1 or 20 mM acetaldehyde or propionaldehyde, 0.4 mM NAD^+, 0.1 mM CoA, 1 mM $MnCl_2$, and 4 μg of BphI−BphJ complex in 100 mM HEPES buffer (pH 8.0). After 5 min, the reaction was quenched with 3 N HCl to pH 5.0 and the mixture filtered through a 0.2 μm filter; 500 μL of sample was subjected to high-pressure liquid chromatography (HPLC) using an AKTA Explorer 100 (Amersham Pharmacia Biotech, Baie d'Urfé, QC) equipped with a reversed-phase Discovery C_{18} column (Supelco). The sample was eluted with a 50 mM phosphate buffer (pH 5.3)/acetonitrile mixture (94:6).

The column flow rate was set at 0.8 mL/min, and CoA esters were detected by absorbance at 254 nm as previously described (*24*). Pure acetyl CoA and propionyl CoA at concentrations ranging from 2 to 100 μM were used as standards.

Pyruvate Proton Exchange Assay. To obtain enzyme samples in deuterated MOPS buffer (pD 8.0), 5 mg of enzyme was concentrated by repeated washing with buffer over an Amicon filtration unit fitted with a YM10 filter. The proton exchange assays were performed in a Bruker Avance 600 MHz spectrometer at 25 °C using a 5.0 mm NMR tube with a 600 μL assay solution containing 0.2 mg of enzyme, 1 mM $MnCl_2$, and 5 mM sodium pyruvate in deuterated MOPS buffer (pD 8.0). NADH was added to one of the samples to a final concentration of 5 mM. Enzyme was added to initiate the reaction, and the ^{1}H NMR spectra was scanned and recorded four times every 3 min over a period of 1 h. A solution without enzyme was measured and used as a negative control. Proton exchange was assessed from the time-dependent change in the ratio of the methyl proton signal of pyruvate (2.38 ppm) to the reference methylene protons at position 1 of MOPS (2.05 ppm) following a previously described method (*12*).

RESULTS

Expression and Purification of the BphI−BphJ Complex. Attempts to separately express and purify BphI and BphJ from recombinant *E. coli* were not successful. BphI formed inclusion bodies, while BphJ irreversibly precipitated out of solution during and after purification. However, coexpression of *bphI* and *bphJ* in *E. coli* using two compatible plasmids (pBTL4 and pET28a, respectively) yielded soluble proteins. BphI and BphJ formed a stable complex as they bind and coelute from the Ni^{2+}-NTA column, although only BphJ has the histidine tag. After purification, the N-terminal histidine tag of BphJ was proteolytically cleaved by thrombin digestion. The typical protein yield per liter of bacterial culture was approximately 8 mg. The purified enzyme can be stored at −80 °C, without loss of activity for at least 12 months.

The molecular masses of BphI and BphJ as estimated by SDS−PAGE are 37 and 32 kDa, respectively, which are in agreement with the predicted molecular mass calculated from the amino acid sequence (Figure 1). The native molecular mass of the purified complex, estimated by gel filtration, was 140 kDa. This corresponds to a heterotetramer with two BphI and two BphJ molecules per complex and is consistent with the subunit arrangements in the crystal structure of the homologous DmpG−DmpF complex (*14*).

Metal Cofactor Preferences and Substrate Specificity of BphI. Specific activities of the aldolase for the substrate 4-hydroxy-2-oxopentanoate were tested using a variety of divalent metal ions at concentrations of 0.1 and 1 mM (Table 1). Cd^{2+} appeared to inhibit the enzyme at the higher concentration (1 mM). The specific activity of the enzyme with Cd^{2+} was highest at a metal ion concentration of 0.01 mM. This specific activity was 79% of the value obtained with Mn^{2+} (1 mM). Since Mn^{2+} gave the highest specific activity and no inhibition was observed with this cation, Mn^{2+} was used as the cofactor for BphI in subsequent analyses.

The specificity of BphI was determined using substrates of varying carbon chain length (Table 2). BphI has similar specificity constants for 4-hydroxy-2-oxopentanoate and the substrate that is one carbon longer, 4-hydroxy-2-oxohexanoate. Although the enzyme can utilize 4-hydroxy-2-oxoheptanoate, specificity is more than 10-fold lower than those of the other two other substrates, due primarily to a low k_{cat} value. The enzyme also exhibited oxaloacetate decarboxylase activity with a k_{cat} more than 3-fold greater than that of the aldol cleavage of 4-hydroxy-2-oxopentanoate. Decarboxylation of oxaloacetate involves C−C bond cleavage, leading to formation of pyruvate and carbon dioxide. The catalytic promiscuity of the enzyme can therefore be rationalized by the common formation of a pyruvate enolate intermediate in both aldolase and decarboxylase reactions. Secondary decarboxylase activity has also been reported for the evolutionarily unrelated pyruvate aldolase, HpaI, which exhibits a decarboxylase activity more than 2-fold greater than the aldolase activity with 4-hydroxy-2-oxopentanoate (*12*).

pH Dependence of BphI Activity and Inhibition by Oxalate. Kinetic parameters for the aldol cleavage of 4-hydroxy-2-oxopentanoate by BphI were determined using constant-ionic strength buffers from pH 6.5 to 9.0. The upper pH limit (pH 9.0) in the activity measurements was due to Mn^{2+} cofactor precipitation. The k_{cat}/K_m and k_{cat} values for the enzyme (Figure 2) showed a single deprotonation with pK_a values of 7.7 ± 0.7 and 7.6 ± 1.3, respectively. These values may reflect the pK_a of a base responsible for the deprotonation of the C4 OH group of the substrate prior to the retro-aldol cleavage reaction. Consistent with the formation of the pyruvate enolate intermediate

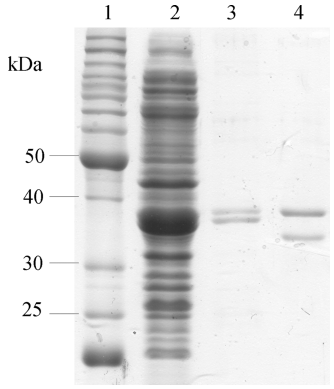

FIGURE 1: Coomassie Blue-stained SDS−polyacrylamide gel of the purified BphI−BphJ complex. Gel loaded with BphI−BphJ samples from crude extract (lane 2), the preparation after Ni^{2+}-NTA column chromatography (land 3), and the preparation after cleavage of the histidine tag (lane 4). The molecular masses of the proteins in the standard (lane 1) are indicated beside the gel. The molecular masses of BphI and BphJ as determined from the gel are 37 and 32 kDa, respectively.

Table 1: Relative Activities of BphI with Various Metal Ions[a]

	relative activity (%)	
metal ion	0.1 mM metal chloride salts	1 mM metal chloride salts
Mn^{2+}	100 ± 3.2	100 ± 4.1
Co^{2+}	19.3 ± 1.3	18.3 ± 1.3
Ni^{2+}	2.6 ± 0.2	17.5 ± 1.0
Mg^{2+}	3.4 ± 0.4	14.8 ± 0.5
Cd^{2+}	56.0 ± 6.4	5.4 ± 1.5

[a] The activity obtained with $MnCl_2$ is taken to be 100% (2.68 and 2.93 units/mg for 0.1 and 1 mM $MnCl_2$, respectively). Assays were performed with 1.78 μg of enzyme, 4 mM 4-hydroxy-2-oxopentanoate, the respective metal chloride salt at 0.1 or 1 mM, 0.4 mM NADH, 19.2 units of LDH, and 100 mM HEPES buffer (pH 8.0) in a total volume of 1 mL.

Table 2: Steady-State Kinetic Parameters of BphI[a]

substrate	K_m (mM)	k_{cat} (s^{-1})	k_{cat}/K_m ($\times 10^4$ M^{-1} s^{-1})
4-hydroxy-2-oxopentanoate	0.22 ± 0.01	4.1 ± 0.5	1.9 ± 0.2
4-hydroxy-2-oxohexanoate	0.18 ± 0.02	3.8 ± 0.2	2.1 ± 0.3
4-hydroxy-2-oxoheptanoate	0.35 ± 0.02	0.63 ± 0.04	0.18 ± 0.01
oxaloacetate	7.5 ± 0.4	16.5 ± 0.5	0.22 ± 0.01

[a]Assays were performed at 25 °C and contained 0.4 mM NADH, 1 mM $MnCl_2$, and 19.2 units of LDH in 100 mM HEPES buffer (pH 8.0) in a total volume of 1 mL.

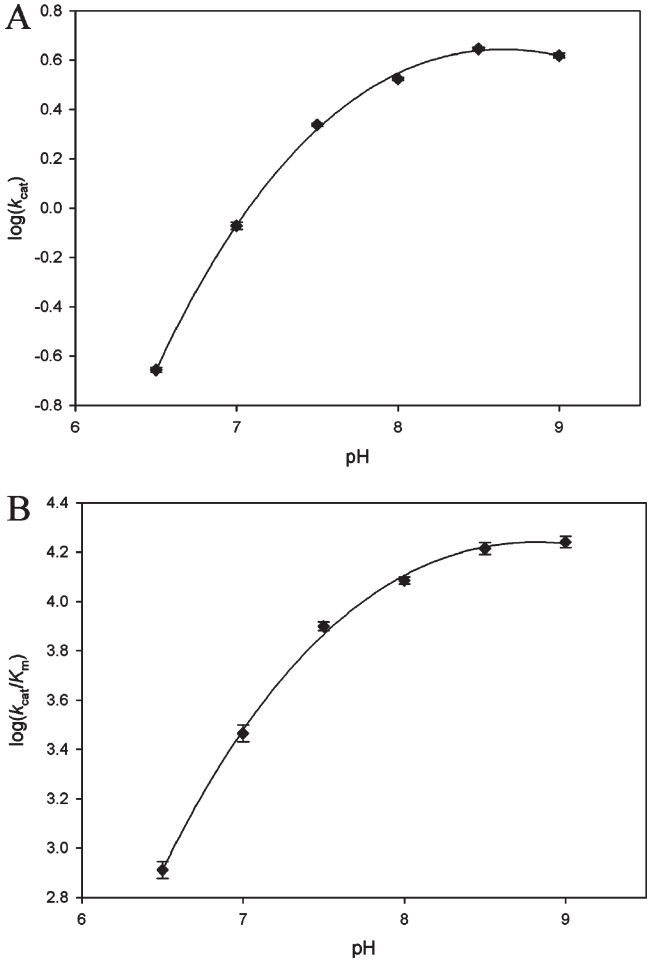

FIGURE 2: pH dependence of k_{cat} and k_{cat}/K_m for BphI. Assay conditions are described in Experimental Procedures. (A) pH dependence of k_{cat}. (B) pH dependence of k_{cat}/K_m. The pK_a values of the catalytic base were determined to be 7.6 ± 1.3 and 7.7 ± 0.7, respectively.

in the reaction mechanism of the aldolase, the stable pyruvate enolate analogue, oxalate, is a potent competitive inhibitor of the aldolase activity, with a K_{ic} of 0.93 ± 0.06 μM (Figure 3).

Substrate and Coenzyme Specificity of BphJ. BphJ was found to be active with a number of hydrophobic aliphatic aldehydes two to five carbons in length (Table 3). The enzyme exhibits broad specificity, with the highest specificity constant obtained for isobutyraldehyde. Interestingly, BphJ does not appear to distinguish between its native substrate, acetaldehyde, and the substrate that is one carbon longer, propionaldehyde, as shown by similar kinetic constants for the two substrates. No activity was detected with succinic semialdehyde, which contains a carboxylic substituent and picolinaldehyde with a pyridine substituent.

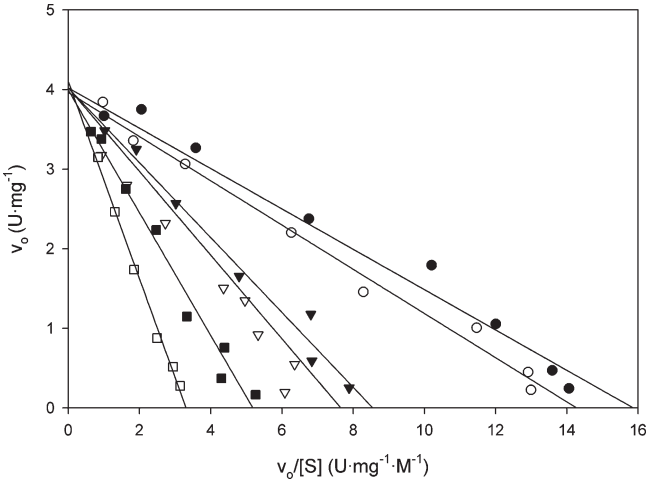

FIGURE 3: Woolf−Augustinsson−Hofstee plot of the inhibition of BphI reaction by oxalate. Assays were performed using 0 (●), 0.2 (○), 0.5 (▼), 1.0 (▽), 2.0 (■), and 4.0 μM oxalate (□) and include 0.4 mM NADH, 1 mM Mn^{2+}, 19.2 units of LDH, 2 μg of enzymes, and 4-hydroxy-2-oxopentanoate at concentrations that varied from at least 0.1K_m to 10K_m, in a total of 1 mL of 100 mM HEPES buffer (pH 8.0). The lines represent the best fit of data to the competitive inhibition equation. The fitted parameters are as follows: K_{ic} = 0.93 ± 0.06 μM, K_m = 0.25 ± 0.01 mM, and k_{cat} = 4.60 ± 0.02 s^{-1}.

Table 3: Steady-State Kinetic Parameters of BphJ with Various Aldehyde Substrates[a]

substrate	$K_{m,app}$ (mM)	k_{cat} (s^{-1})	$k_{cat}/K_{m,app}$ ($\times 10^2$ M^{-1} s^{-1})
acetaldehyde	23.6 ± 1.8	17.2 ± 0.5	7.3 ± 0.06
propionaldehyde	23.1 ± 1.7	16.3 ± 0.5	7.0 ± 0.05
butyraldehyde	31.7 ± 2.2	9.5 ± 0.2	3.0 ± 0.02
isobutyraldehyde	7.7 ± 0.5	11.2 ± 0.3	14.0 ± 0.1
pentaldehyde[b]	ND[c]	ND[c]	0.76[b]

[a]Assays were performed at 25 °C and contained 0.4 mM NAD^+ and 0.1 mM coenzyme A in 100 mM HEPES buffer (pH 8.0) in a total volume of 1 mL. [b]Due to low substrate solubility and the high apparent K_m for this substrate, the specificity constant can be estimated from only the gradient of the specific activity vs substrate concentration graph. [c]Not determined.

BphJ was able to utilize both NAD^+ and $NADP^+$ with comparable k_{cat} values (Table 4). However, the apparent K_m for NAD^+ is 16-fold lower than for $NADP^+$.

Substrate Channeling. Substrate channeling was assessed using two methods. First, the substrate of BphI, 4-hydroxy-2-oxopentanoate, was added to the BphI−BphJ complex, and the BphJ activity was determined spectroscopically on the basis of reduction of NAD^+. If substrate channeling does not occur, then a lag phase in the BphJ progress curve will be observed that corresponds to the time taken for the concentration of acetaldehyde to reach the steady-state level. On the basis of eq 2, this lag

Table 4: Steady-State Kinetic Parameters of BphJ with Different Nicotinamide Cofactors[a]

substrate	$K_{m,app}$ (μM)	k_{cat} (s^{-1})	$k_{cat}/K_{m,app}$ ($\times 10^5$ M^{-1} s^{-1})
NAD^+	34.8 ± 1.9	14.1 ± 0.2	4.0 ± 0.02
$NADP^+$	561 ± 21	12.9 ± 0.2	0.22 ± 0.01

[a]Assays were performed at 25 °C and contained 100 mM acetaldehyde and 0.1 mM coenzyme A in 100 mM HEPES buffer (pH 8.0) in a total volume of 1 mL.

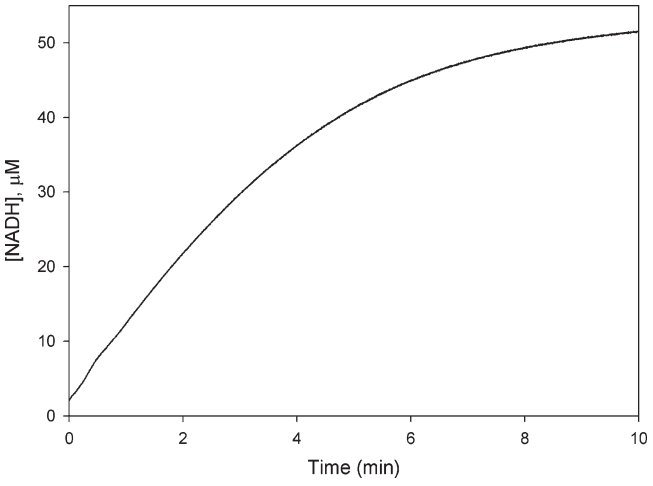

FIGURE 4: Progress curve for NADH formation in the coupled aldolase and dehydrogenase assay. Reactions were performed as described in Experimental Procedures. No lag was visualized when the coupled assay was initiated with the BphI−BphJ complex.

time is estimated to be 3100 min due to the high apparent K_m of acetaldehyde for BphJ. However, the experimentally determined progress curve showed no lag time (Figure 4). In addition, the activity of BphJ estimated from the progress curve is 10.4 s^{-1}, which is ~60% of the k_{cat} value for BphJ determined using exogenous acetaldehyde, even though the theoretical maximum concentration of acetaldehyde produced by aldol cleavage of 4-hydroxy-2-oxopentanoate in the assay is only 0.1 mM, 236-fold lower than the apparent K_m of acetaldehyde for BphJ. Therefore, the activity of BphJ corresponds to an acetaldehyde concentration 360-fold higher than expected from the maximum acetaldehyde produced from the assay. A similar progress curve, without a lag phase, was also observed when NAD^+ was substituted with $NADP^+$ for the BphJ reaction.

We also took advantage of the fact that BphJ has similar steady-state kinetic parameters for acetaldehyde and propionaldehyde, to assess substrate channeling using a competing substrates method. Exogenous propionaldehyde is provided in a 10-fold molar excess concentration over 4-hydroxy-2-oxopentanoate in a BphI−BphJ coupled assay where coenzyme A is limiting. If no substrate channeling occurs, the excess propionaldehyde can effectively compete with acetaldehyde released from BphI, resulting in predominantly propionyl CoA formation in the BphJ reaction. However, HPLC analysis of reaction products revealed formation of 65 μM acetyl CoA and only 3.2 μM propionyl CoA (Figure 5). Conversely, using 4-hydroxy-2-oxohexanoate instead of 4-hydroxy-2-oxopentanoate, and acetaldehyde instead of propionaldehyde as the exogenous competing substrate, 68 μM propionyl CoA and 0.72 μM acetyl CoA were produced, demonstrating that propionaldehyde can also be directly channeled from the aldolase to the dehydrogenase. When the concentrations of

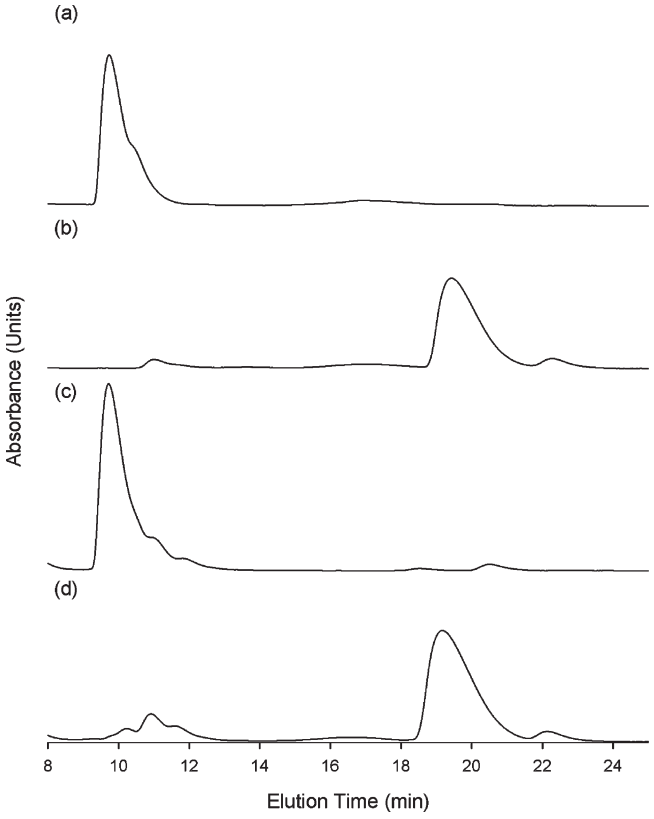

FIGURE 5: HPLC traces of reaction mixtures. Samples were loaded onto a C_{18} column and eluted with a 50 mM phosphate buffer (pH 5.3)/acetonitrile mixture (94:6). CoA esters were detected by absorbance at 254 nm: (a) 50 μM acetyl CoA, (b) 50 μM propionyl CoA, (c) products of the BphI−BphJ reaction mixture containing 0.1 mM 4-hydroxy-2-oxopentanoate and 1 mM propionaldehyde, and (d) products of the BphI−BphJ reaction mixture containing 0.1 mM 4-hydroxy-2-oxohexanoate and 1 mM acetaldehyde.

the competing exogenous aldehydes were increased to 20 mM, which is near the K_m values for these aldehydes in BphJ, significant amounts of channeled products were still produced, constituting ~30% of the total CoA esters formed, even though exogenous competing aldehydes are in 200-fold molar excess over the aldolase substrates (0.1 mM) in these assays.

Allosteric Regulation of BphI by BphJ. Activity of BphI was estimated when acetaldehyde turnover was occurring in BphJ. The activity of BphI determined by a discontinuous assay in this reaction was found to be 12.0 μmol min^{-1} mg^{-1}, which represents an ~15-fold increase in activity over the aldolase activity when no catalysis is occurring in BphJ.

Kinetic parameters for BphI were also determined in the presence of various coenzymes of BphJ (Table 5). The presence of NAD^+, $NADP^+$, NADH, or CoA led to an at least 5-fold reduction in the K_m of BphI for 4-hydroxy-2-oxopentanoate. Furthermore, 2- and 5-fold increases in k_{cat} were observed when the BphI reaction was conducted in the presence of NAD^+ and NADH, respectively. Overall, the highest catalytic efficiency (k_{cat}/K_m) of BphI occurred when NADH is present, which is 25-fold higher than the value obtained without nucleotides.

The pyruvate proton exchange half-reaction of the aldolase reaction was also determined in the presence and absence of NADH using proton NMR, which gave values of 0.44 ± 0.02 and 0.36 ± 0.01 μmol min^{-1} mg^{-1}, respectively. This indicates that NADH activation of BphI activity is not due to the increased pyruvate proton exchange rate.

Table 5: Kinetic Parameters of BphI for 4-Hydroxy-2-oxopentanoate in the Presence of Various Nucleotides[a]

cofactor	K_m (mM)	k_{cat} (s^{-1})	k_{cat}/K_m ($\times 10^3$ M^{-1} s^{-1})
no nucleotides	1.12 ± 0.11	0.87 ± 0.02	0.78 ± 0.07
CoA	0.15 ± 0.02	0.78 ± 0.01	5.25 ± 0.37
NAD^+	0.23 ± 0.11	1.75 ± 0.04	7.65 ± 0.76
$NADP^+$	0.11 ± 0.01	0.66 ± 0.01	5.90 ± 0.43
NADH	0.22 ± 0.01	4.1 ± 0.5	18.6 ± 2.0

[a]Assays were performed at 25 °C and contained 80 μg of enzyme, 1 mM $MnCl_2$, and 0.4 mM CoA, NAD^+, and NADH or 2 mM $NADP^+$ in 8 mL of 100 mM sodium HEPES buffer (pH 8.0). Kinetic parameters for NADH were determined directly using the standard continuous assay, while discontinuous assays were performed with the other nucleotides.

DISCUSSION

The aldolase and dehydrogenase complex from the *meta* cleavage pathway of various aromatics is important for the production of metabolites that can enter central metabolic pathways. While the crystal structure of the enzyme complex (DmpG−DmpF) from the phenol degradation pathway is available (*14*), detailed kinetic analysis of the enzymes, substrate specificity constant determination, or biochemical evidence of substrate channeling has not been reported. Here, the BphI−BphJ complex from the PCB degradation pathway was purified and characterized, providing important biochemical insight into this family of aldolase and dehydrogenase enzymes. In the *bph* pathway, 4-hydroxy-2-oxopentanoate is produced from biphenyl and is converted by the aldolase, BphI, to pyruvate and acetaldehyde. The latter is then transformed by BphJ to acetyl CoA. In contrast, the *meta* cleavage pathway for other aromatics, such as cholesterol, yields 4-hydroxy-2-oxohexanoate, which is then cleaved to form pyruvate and propionyl CoA (*1*). BphI and BphJ did not appear to discriminate between 4-hydroxy-2-oxopentanoate or 4-hydroxy-2-oxohexanoate and acetaldehyde or propionaldehyde, respectively, as they are able to transform these metabolites that differ by one carbon in length with equal catalytic efficiency.

Besides its aldolase activity, BphI is able to catalyze the decarboxylation of oxalocaetate and is inhibited by oxalate, providing evidence of a catalytic mechanism involving the formation of a pyruvate enolate intermediate. In this regard, it is similar to another pyruvate aldolase HpaI, from the catabolic pathway of hydroxyphenylacetate, although BphI and HpaI are unrelated in structure or sequence and appear to have evolved independently to catalyze similar reactions. The natural substrate of HpaI is 4-hydroxy-2-oxoheptane-1,7-dioate which is transformed to pyruvate and succinic semialdehyde, although it also has high activity for 4-hydroxy-2-oxopentanoate (353 s^{-1}), the substrate of BphI (*12*). There are, however, some notable differences in properties between the two enzymes. BphI has the highest specific activity with Mn^{2+} as a cofactor, while HpaI utilizes Mn^{2+} and Co^{2+} with equal efficiency (*12*). The pK_a of the catalytic base in BphI was found to be ~7.7, whereas in HpaI, the pK_a of the base (identified as a histidine residue) is 6.8 (*11*). Finally, while BphI is closely associated with another enzyme, BphJ, HpaI exists as a homohexamer (*13*).

The close association of enzymes with distinct catalytic activities may allow for the synchronization of chemical reactions and the efficient transfer of common metabolites within the enzyme complex. This is exemplified by the bifunctional enzyme, tryptophan synthase. The α subunit of this enzyme catalyzes the cleavage of 3-indole-D-glycerol 3′-phosphate to glyceraldehyde 3-phosphate and indole. The chemically labile indole product is then directly channeled via a 25 Å long molecular tunnel to the β subunit where it condenses with L-serine to form L-tryptophan (*25*−*27*). In the BphI−BphJ complex, transit time analysis and substrate competition assays provide the first evidence that substrate channeling also occurs in this enzyme complex. Aldehydes are reactive compounds that are toxic since they can modify cellular biomolecules. Given the high apparent K_m values for aldehydes in BphJ and the toxicity of aldehydes, it is unlikely that exogenous aldehydes can accumulate to sufficiently high concentrations to allow the enzyme to operate near V_{max} without detrimental effects to the cell. The fact that acetaldehyde and propionaldehyde are directly channeled from BphI to BphJ ensures that these toxic aldehydes are sequestered from cellular components. This also increases the effective concentration of aldehydes experienced by BphJ, allowing it to catalyze the reaction near its maximum catalytic rate. It is interesting to note that in tryptophan synthase, exogenous indole can compete effectively with channeled indole in the β reaction, suggesting that exogenous indole may enter the β site through the same channel that links the active sites of the two subunits (*27*). In contrast, our substrate competition assays with the BphI−BphJ complex showed that exogenous aldehyde cannot compete with the channeled aldehyde in the BphJ reaction, indicating that it did not enter BphJ through the channel from BphI.

Enzymes that exhibit substrate channeling are often allosterically regulated, ensuring that the reactions occurring in separate active sites are coupled. For example, in tryptophan synthase, binding of L-serine at the β site increases the cleavage rate of 3-indole-D-glycerol 3′-phosphate at the α site by 30-fold (*27*, *28*). This ensures that the coreactant (L-serine) is available to react with indole produced and channeled from the α site. Likewise, in carbamoyl phosphate synthetase, formation of a carboxy phosphate intermediate triggers hydrolysis of glutamine to release ammonia which is then channeled to react with carbamoyl phosphate (*29*). Binding of ATP and the consequent reaction with bicarbonate within the large subunit also increase the overall rate of hydrolysis of glutamine by 3 orders of magnitude (*30*). We observed that BphI specific activity increased by 15-fold when BphJ underwent turnover, suggesting an allosteric mechanism in which the dehydrogenase activates the aldolase. Hydrogen−deuterium exchange analysis of the homologous dehydrogenase, DmpF, showed that NAD^+ and CoA bind on the same site in the dehydrogenase structure, consistent with a proposed ping-pong kinetic mechanism, whereby alternate binding of NAD^+ and CoA to the dehydrogenase allows for the oxidation of a thiohemiacetal intermediate formed between a proposed catalytic cysteine and the aldehyde and the subsequent production of acetyl CoA (*31*). While CoA and nicotinamide cofactors lowered the K_m of BphI for 4-hydroxy-2-oxopentanoate, it is interesting that only NAD^+ and NADH were able to increase the k_{cat} value, with the highest increase in k_{cat} observed with NADH, the product of the BphJ reaction. Further analysis revealed that the pyruvate proton transfer rate in BphI is unaltered in the presence of NADH, suggesting that activation of the aldol reaction by NADH occurred prior to this step, possibly in the base-catalyzed abstraction of the C4 hydroxyl group of the substrate. Overall, production of NADH in BphJ can account for only one-third of the activation of BphI observed during BphJ turnover, suggesting that other intermediates in the BphJ reaction or dynamic motion during BphJ catalysis are important for allosteric regulation of BphI activity.

In conclusion, the biochemical and kinetic characterization of the BphI−BphJ complex presented should form a strong basis for future structure−function studies aimed at elucidating mechanisms of channeling and regulation in this interesting enzyme complex.

ACKNOWLEDGMENT

We thank Joe Meissner from the University of Guelph for guidance in the acquisition of NMR spectra.

REFERENCES

(1) Van der Geize, R., Yam, K., Heuser, T., Wilbrink, M. H., Hara, H., Anderton, M. C., Sim, E., Dijkhuizen, L., Davies, J. E., Mohn, W. W., and Eltis, L. D. (2007) A gene cluster encoding cholesterol catabolism in a soil actinomycete provides insight into *Mycobacterium tuberculosis* survival in macrophages. *Proc. Natl. Acad. Sci. U.S.A. 104*, 1947–1952.

(2) de Chastellier, C., and Thilo, L. (2006) Cholesterol depletion in *Mycobacterium avium*-infected macrophages overcomes the block in phagosome maturation and leads to the reversible sequestration of viable mycobacteria in phagolysosome-derived autophagic vacuoles. *Cell. Microbiol. 8*, 242–256.

(3) Pieters, J., and Gatfield, J. (2002) Hijacking the host: Survival of pathogenic mycobacteria inside macrophages. *Trends Microbiol. 10*, 142–146.

(4) Furukawa, K., and Kimura, N. (1995) Biochemistry and genetics of PCB metabolism. *Environ. Health Perspect. 103* (Suppl. 5), 21–23.

(5) Diaz, E. (2004) Bacterial degradation of aromatic pollutants: A paradigm of metabolic versatility. *Int. Microbiol. 7*, 173–180.

(6) Furukawa, K., Hirose, J., Suyama, A., Zaiki, T., and Hayashida, S. (1993) Gene components responsible for discrete substrate specificity in the metabolism of biphenyl (bph operon) and toluene (tod operon). *J. Bacteriol. 175*, 5224–5232.

(7) Furukawa, K., Simon, J. R., and Chakrabarty, A. M. (1983) Common induction and regulation of biphenyl, xylene/toluene, and salicylate catabolism in *Pseudomonas paucimobilis*. *J. Bacteriol. 154*, 1356–1362.

(8) Narayanan, B. C., Niu, W., Han, Y., Zou, J., Mariano, P. S., Dunaway-Mariano, D., and Herzberg, O. (2008) Structure and function of PA4872 from *Pseudomonas aeruginosa*, a novel class of oxaloacetate decarboxylase from the PEP mutase/isocitrate lyase superfamily. *Biochemistry 47*, 167–182.

(9) Schmitzberger, F., Smith, A. G., Abell, C., and Blundell, T. L. (2003) Comparative analysis of the *Escherichia coli* ketopantoate hydroxymethyltransferase crystal structure confirms that it is a member of the $(\beta\alpha)_8$ phosphoenolpyruvate/pyruvate superfamily. *J. Bacteriol. 185*, 4163–4171.

(10) Forouhar, F., Hussain, M., Farid, R., Benach, J., Abashidze, M., Edstrom, W. C., Vorobiev, S. M., Xiao, R., Acton, T. B., Fu, Z., Kim, J. J., Miziorko, H. M., Montelione, G. T., and Hunt, J. F. (2006) Crystal structures of two bacterial 3-hydroxy-3-methylglutaryl-CoA lyases suggest a common catalytic mechanism among a family of TIM barrel metalloenzymes cleaving carbon-carbon bonds. *J. Biol. Chem. 281*, 7533–7545.

(11) Wang, W., and Seah, S. Y. (2008) The role of a conserved histidine residue in a pyruvate-specific class II aldolase. *FEBS Lett. 582*, 3385–3388.

(12) Wang, W., and Seah, S. Y. (2005) Purification and biochemical characterization of a pyruvate-specific class II aldolase, HpaI. *Biochemistry 44*, 9447–9455.

(13) Rea, D., Fulop, V., Bugg, T. D., and Roper, D. I. (2007) Structure and mechanism of HpcH: A metal ion dependent class II aldolase from the homoprotocatechuate degradation pathway of *Escherichia coli*. *J. Mol. Biol. 373*, 866–876.

(14) Manjasetty, B. A., Powlowski, J., and Vrielink, A. (2003) Crystal structure of a bifunctional aldolase-dehydrogenase: Sequestering a reactive and volatile intermediate. *Proc. Natl. Acad. Sci. U.S.A. 100*, 6992–6997.

(15) Sambrook, J., Fritsch, E. F., and Maniatis, T. (1989) Molecular cloning: A laboratory manual , Cold Spring Harbor Laboratory Press, Plainview, NY.

(16) Hofer, B., Backhaus, S., and Timmis, K. N. (1994) The biphenyl/polychlorinated biphenyl-degradation locus (bph) of *Pseudomonas sp*. LB400 encodes four additional metabolic enzymes. *Gene 144*, 9–16.

(17) Tabor, S., and Richardson, C. C. (1985) A bacteriophage T7 RNA polymerase/promoter system for controlled exclusive expression of specific genes. *Proc. Natl. Acad. Sci. U.S.A. 82*, 1074–1078.

(18) Lynch, M. D., and Gill, R. T. (2006) Broad host range vectors for stable genomic library construction. *Biotechnol. Bioeng. 94*, 151–158.

(19) Chain, P. S., Denef, V. J., Konstantinidis, K. T., Vergez, L. M., Agullo, L., Reyes, V. L., Hauser, L., Cordova, M., Gomez, L., Gonzalez, M., Land, M., Lao, V., Larimer, F., LiPuma, J. J., Mahenthiralingam, E., Malfatti, S. A., Marx, C. J., Parnell, J. J., Ramette, A., Richardson, P., Seeger, M., Smith, D., Spilker, T., Sul, W. J., Tsoi, T. V., Ulrich, L. E., Zhulin, I. B., and Tiedje, J. M. (2006) *Burkholderia xenovorans* LB400 harbors a multi-replicon, 9.73-Mbp genome shaped for versatility. *Proc. Natl. Acad. Sci. U.S.A. 103*, 15280–15287.

(20) Bradford, M. M. (1976) A rapid and sensitive method for the quantitation of microgram quantities of protein utilizing the principle of protein-dye binding. *Anal. Biochem. 72*, 248–254.

(21) Laemmli, U. K. (1970) Cleavage of structural proteins during the assembly of the head of bacteriophage T4. *Nature 227*, 680–685.

(22) Cornish-Bowden, A. (1995) Analysis of enzyme kinetic data , Oxford University Press, New York.

(23) Easterby, J. S. (1973) Coupled enzyme assays: A general expression for the transient. *Biochim. Biophys. Acta 293*, 552–558.

(24) Powlowski, J., Sahlman, L., and Shingler, V. (1993) Purification and properties of the physically associated meta-cleavage pathway enzymes 4-hydroxy-2-ketovalerate aldolase and aldehyde dehydrogenase (acylating) from *Pseudomonas* sp. strain CF600. *J. Bacteriol. 175*, 377–385.

(25) Dunn, M. F., Aguilar, V., Brzovic, P., Drewe, W. F.Jr., Houben, K. F., Leja, C. A., and Roy, M. (1990) The tryptophan synthase bienzyme complex transfers indole between the α- and β-sites via a 25−30 Å long tunnel. *Biochemistry 29*, 8598–8607.

(26) Lane, A. N., and Kirschner, K. (1991) Mechanism of the physiological reaction catalyzed by tryptophan synthase from *Escherichia coli*. *Biochemistry 30*, 479–484.

(27) Anderson, K. S., Miles, E. W., and Johnson, K. A. (1991) Serine modulates substrate channeling in tryptophan synthase. A novel intersubunit triggering mechanism. *J. Biol. Chem. 266*, 8020–8033.

(28) Brzovic, P. S., Ngo, K., and Dunn, M. F. (1992) Allosteric interactions coordinate catalytic activity between successive metabolic enzymes in the tryptophan synthase bienzyme complex. *Biochemistry 31*, 3831–3839.

(29) Miles, B. W., and Raushel, F. M. (2000) Synchronization of the three reaction centers within carbamoyl phosphate synthetase. *Biochemistry 39*, 5051–5056.

(30) Miles, B. W., Banzon, J. A., and Raushel, F. M. (1998) Regulatory control of the amidotransferase domain of carbamoyl phosphate synthetase. *Biochemistry 37*, 16773–16779.

(31) Lei, Y., Pawelek, P. D., and Powlowski, J. (2008) A shared binding site for NAD^+ and coenzyme A in an acetaldehyde dehydrogenase involved in bacterial degradation of aromatic compounds. *Biochemistry 47*, 6870–6882.